FRA winding type field cases and automatic classification using AI

Using machine learning to validate and identify SFRA characteristics

ABSTRACT

Artificial intelligence is a very powerful tool to bundle expert knowledge into algorithms. This helps in providing expert knowledge on demand. In the further course, the authors want to give some examples of how powerful AI in the analysis of SFRA curves and checking the quality and validity already is. Furthermore, a proposal for the sub-band separation is discussed, and some field cases are presented.

KEYWORDS:

artificial intelligence, gradient-boosting algorithm, machine learning, measurement quality, measurement validation, pattern recognition, power transformer, SFRA

Jean SANCHEZ, David GOPP

Power transformers are critical to all High Voltage networks and are quite reliable over the long term, with a typical failure rate of around 1 % or less

Grounding capacitance is greater near the locations where the winding is near to the ground (i.e. the core, the tank, earth shield, if any), whereas serial capacitance is majorly influenced by the winding design

1. Introduction

Power transformers are critical to all High Voltage (HV) networks and are quite reliable over the long term, with a typical failure rate of around 1 % or less [1]. The CIGRE Working Group (WG) A2.49 has elaborated that offline as well as online monitoring and operational data are crucial factors for condition-based transformer assessment [2]. The quality of the data plays a viable role so that the right conclusions can be drawn from it. This includes both the acquisition and the processing of data. The SFRA method is one of several offline methods which is commonly used and has shown to be the most sensitive and non-invasive method to detect mechanical, especially electrical, faults. More specifically, the mechanical integrity of the core, windings, and clamping structure as well as the electrical integrity, such as shorted windings and turns. [3] To improve its diagnosis, artificial intelligence tools are tried to be used, like interesting proposals of [4] §6.4, to automate at best diagnosis firstly and somehow better understand winding designs, mostly unknown to the final clients, and then its faults in future works. This paper tries to assess winding design through FRA field cases by knowing some of it from manufacturers and to give new ways of automatically assessing FRA curves from the field as often difficult, especially for non-experts.

2. Winding designs

Power transformers' active part is made of windings, manually manufactured for all ratings above a few MVA. The design challenges on windings are to carry the current and to withstand the high voltage and its transients. Two main winding designs are now used in the world, core type and shell "pancake" type designs (under Westinghouse license, historically), with significantly different geometry. Both types are working well, even if the core type is more widely manufactured in the world than the shell type, and both are subject to the same challenges.

To carry significant current and minimize additional load losses, by stray losses effect in the winding itself for the most part, it is necessary to split the copper cross-section into smaller parallel sections. If the area of each copper conductor in front of the leakage flux is minimized, then the stray losses could be somehow optimized. With some limitations linked to the mechanical withstand of short-circuit forces. On the other hand, to limit circulations currents, associated losses, and the local abnormal temperature rises, over any wide windings, some permutations of elementary conductors could be performed so that any single conductor of any winding would let pass more or less the same leakage flux.

Finally, one of the highest stresses to withstand then is the lightning impulse, a fast transient of very high voltage. In such cases, most of those transient "passes" through the windings by capacitance effects and not by inductance effect. Then to improve those capacitive voltage transfers, different winding designs have been developed by different factories in the world to improve the "serial" (Cs) and "grounding" capacitances that are significant in this matter. Grounding capacitance is greater near the locations where the winding is near the ground (i.e. the core, the tank, earth shield, if any), whereas serial capacitance is majorly influenced by the winding design.

Today three main windings' designs could be listed: continuous, or "plain" (disc, as in Fig. 1 [5], layer or helical for core types), interleaved with cross-links between individual conductors (for core types), or with Continuously Transposed Conductors (CTCs), see [6] §4.5.3.

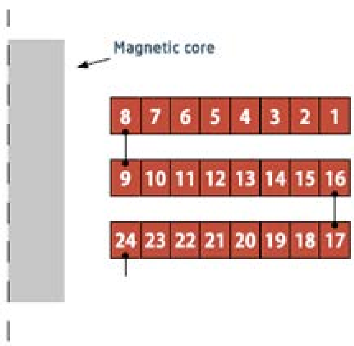

Figure 1. A continuous disc winding [5]

In 1947, a particularly interleaved conductor design on core type discs was patented in England in "The English Electric Company" by George Fletcher Stearn, "a British subject, of Siemens Works, Stafford" (today GE) [7] and then widely used by many manufacturers. A typical scheme from the original patent is shown in Fig. 2, with the numbers listed to follow the electric circuit. A point to note is that some brazing is needed at every two discs, at least.

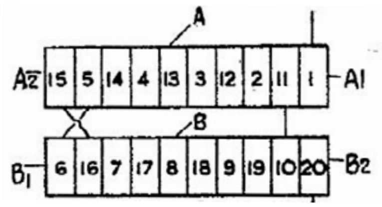

Figure 2. Original patent scheme of an interleaved design [7]

There are also shielded discs [5] with "floating screens" between some turns for further improvement of serial capacitance to better withstand lightning impulses.

CTCs are of different sizes of elementary conductors, quite efficient but expansive, and they could be thick and tough to wind.

A combination of different winding designs is possible on one winding. Generally, "advanced" designs, like interleaved, on the line part, which is the most stressed by voltage transient, then "classical" designs, like continuous for the rest of the winding, and an often different one for the tap winding, like helical [5].

Consequently, most power transformer winding designs in use today are not known by the final user, and this is almost impossible to guess without forensic investigation

> **Based on the EDF FRA database, mostly on Factory Acceptance Tests and some onsite investigations tests, some winding design types can be determined**

Most of the time, CTC windings are only with CTC. As usual in transformers, exceptions may always exist.

Winding design is the manufacturer's choice, based on each industrial experience, and could be somehow different over a long time and manufacturer. And the winding design is seldom given or explained to the final customer, especially if the transformer passes its final tests and meets its original specifications.

Consequently, most power transformer winding designs in use today are not known by the final user, and this is almost impossible to guess without forensic investigation.

FRA tests are somehow sensitive to winding designs, and this paper tries to understand and show, partly from experience, how winding design could influence those measurements.

3. SFRA sub-bands dominated by the winding–field cases

One unique example is given in Fig. 3 from [4], where different winding designs have been identified on FRA in literature, which could be seen between 10 kHz and 1 MHz. The interleaved disc is rather smooth compared to plain disc winding, with many resonances in the medium frequency range more sensitive to windings.

Based on the EDF FRA database, mostly on Factory Acceptance Tests (FAT) and some onsite investigations tests, some winding design types can be determined and reported to the final utility.

Following are some examples based on 21 analyzed cases on Generator Step-Up (GSU) transformers ranging from 72 to 420 kV classes and from 20 to 600 MVA, which can be better understood with the visual aid if some trends between winding designs and FRA curves are possible. The interesting part here happens above 10 kHz, typically where the wind has the highest influence on FRA curves.

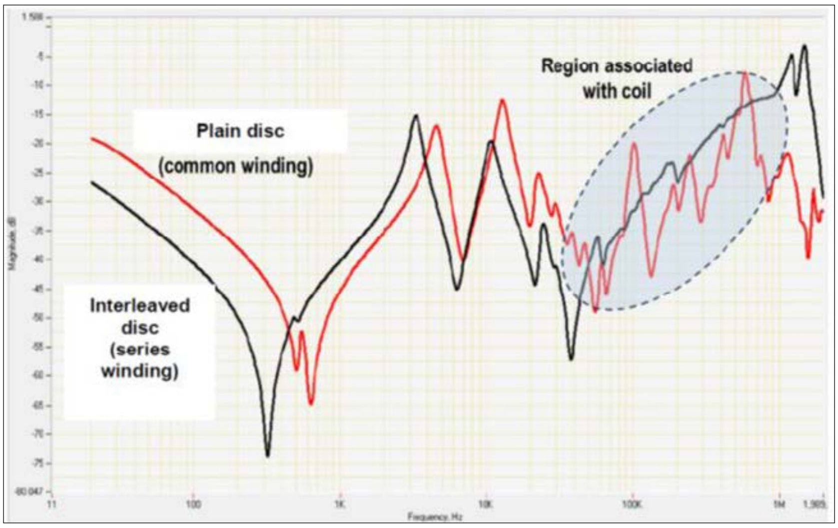

Figure 3. An example of FRA difference between two winding designs: plain and interleaved discs [4]

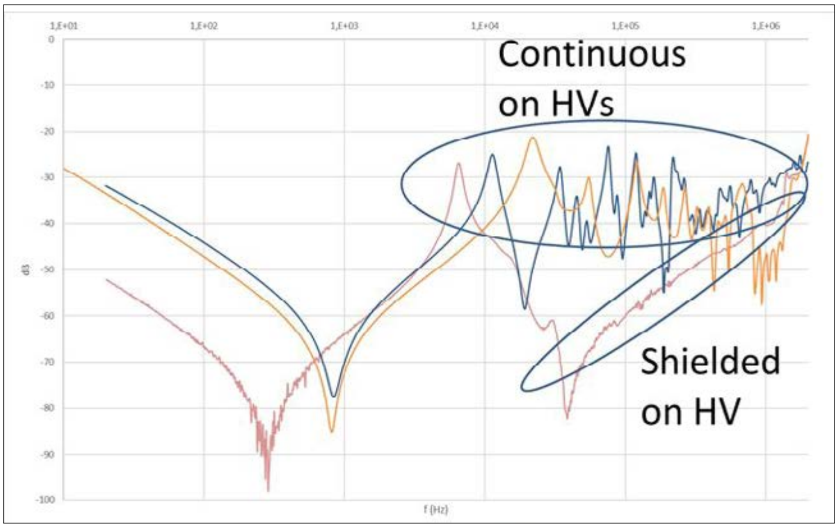

Figure 4. FRA on HV continuous and shielded discs designs

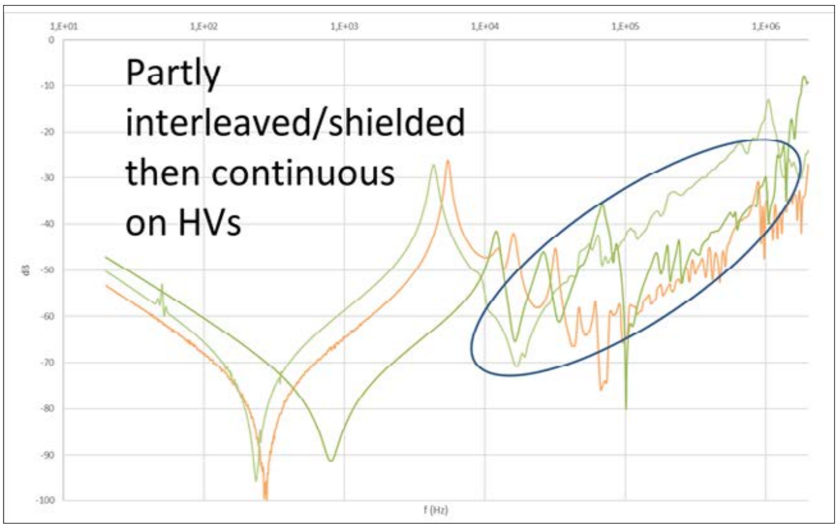

Figure 5. FRA on HV partially interleaved or shielded online then continuous designs

Artificial Intelligence (AI) in any application is not present only in the model itself but also in using even a larger amount of data for the prediction task

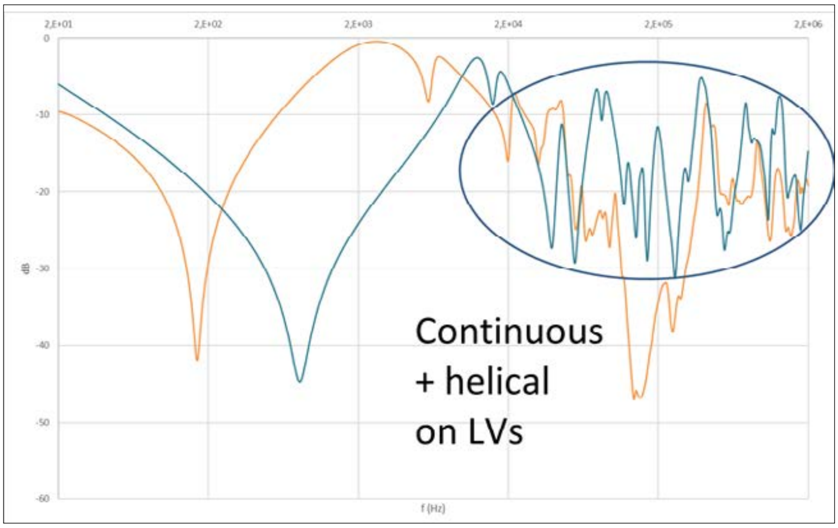

Figure 6. FRA on LV with continuous and helical designs

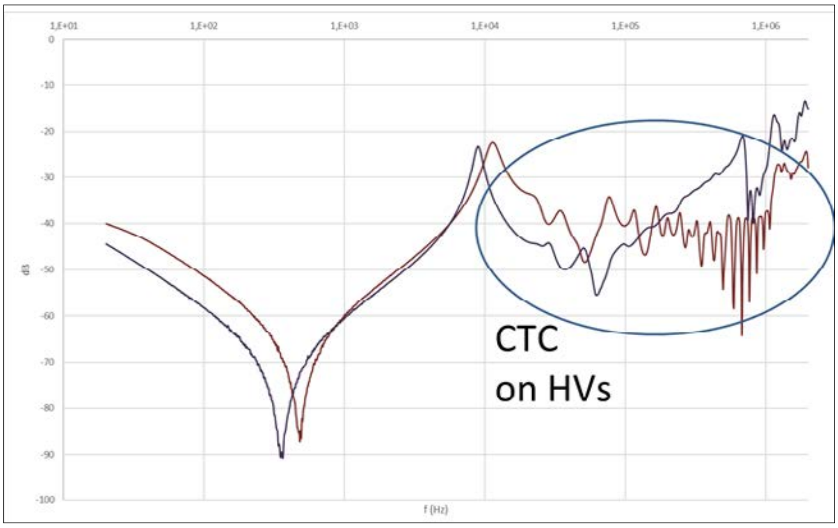

Figure 7. FRA on HV with CTC design

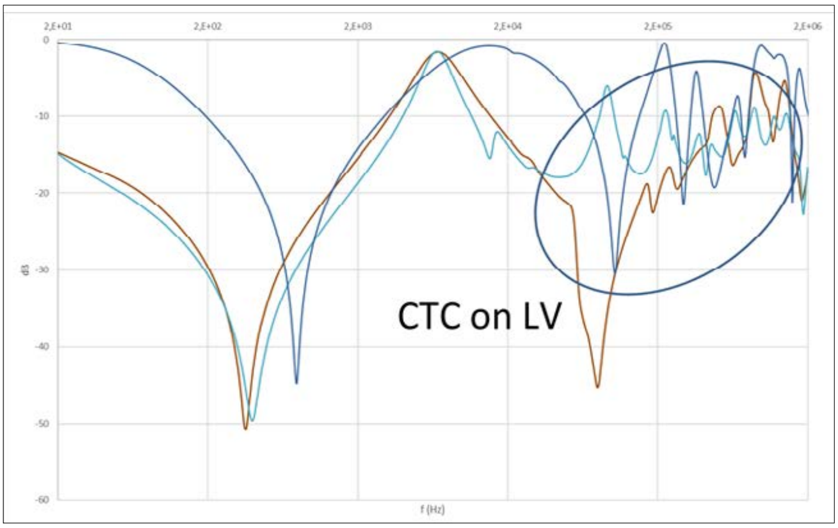

Figure 8. FRA on LV with CTC design

HV and LV curves have been separated, and just a few significant curves have been chosen for visual clarity.

In Fig. 4, we confirm the CIGRE example, with a smooth curve, we have an "upper trend" with shielded discs designed on HV, compared to continuous / plain discs with more resonances and being "flatter".

In Fig. 5, three HV designs are partly wound with interleaved, or shielded, designs on the line, still to improve lighting impulses, then continuous "classic" design. What could be, somehow, seen is an "upper trend", which could be due to the interleaved / shielded designs, with more resonances than the previous full shielded discs example, which could be due to the continuous design.

In Fig. 6, on LV sides, continuous and helical designs [5] are shown, still with many resonances. The helical design could be seen as a specific continuous design without any special capacitance effect to withstand lightning impulses.

In Fig. 7 and Fig. 8, CTC wound HV and LV show that we could get different kinds of curves with many resonances – or less (in Fig. 7). Then, it is rather hard to link CTC winding type to FRA curves.

It is particularly hard to link the winding design not knowing the FRA curves.

Anyhow, serial capacitance effects like interleaved and shielded windings seem to smooth and give an "upper trend" on HV. When continuous "classic" designs show more resonance and a somewhat "flatter" trend, such as helical winding, it could be somehow close in terms of capacitance. Finally, CTCs designs give no clear trends on FRA curves at the first analysis.

Maybe in future, some machine learning of digital analysis could deepen this winding design effect into consideration for further assessment analysis.

4. Automatic validation of SFRA measurement results

Data quality and validity will be one of many crucial factors in this century when deriving information from raw data for further digital assessment. Furthermore, the highest potential for optimizing prediction results when using Artificial Intelligence (AI) in any application is not present only in the model itself but also in using even a larger amount of data for the prediction task. Fig. 9 indicates the steps that are necessary for deriving a piece of information about the assessment of a power transformer test from raw data. This can be done either automatically or manually by experts.

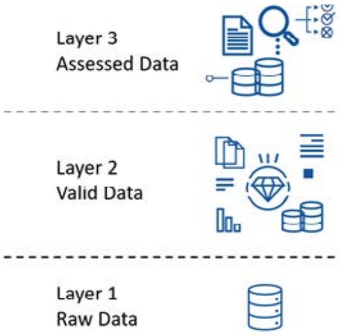

Figure 9. Data levels

The CIGRE WG A2.26 [8], followed later by the WG A2.53 [4], discussed seven influencing factors regarding the influence of the test setup: the test voltage, the direction of end-to-end measurements, earthing neutral bushing in the not-under-test winding, a connection between the shield of the test lead, poor connections of short-circuit cables, external busbar on bushings and poor grounding.

The automatic validation includes a prediction for the respective SFRA pattern and the automatic detection, respectively, classification of:

- Noise (nominal / harmonic noise, Fig. 10, and noise caused by the measuring device, Fig. 11).
- The state of the transformer in terms of residual frequency magnetism, Table 1.

On the one hand, there is noise occurring around the rated frequency / harmonic frequencies, and on the other hand, there is noise caused by the dynamic range of the measuring device

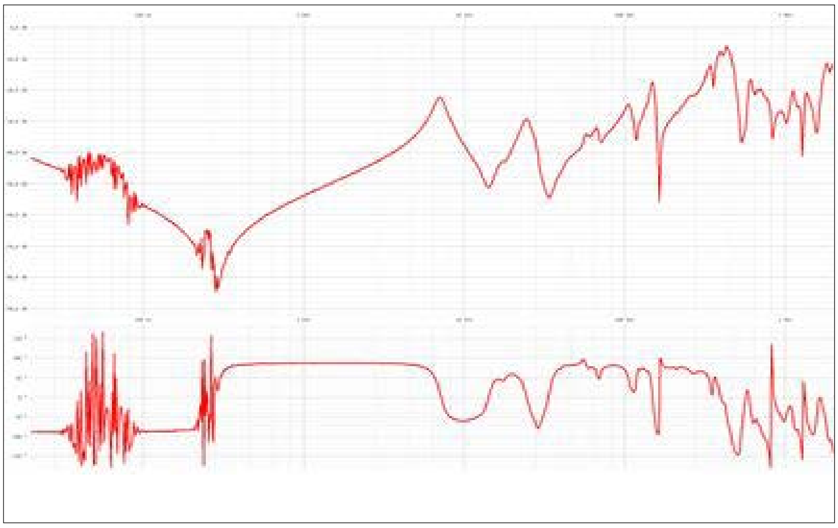

Figure 10. Effect of external interferences

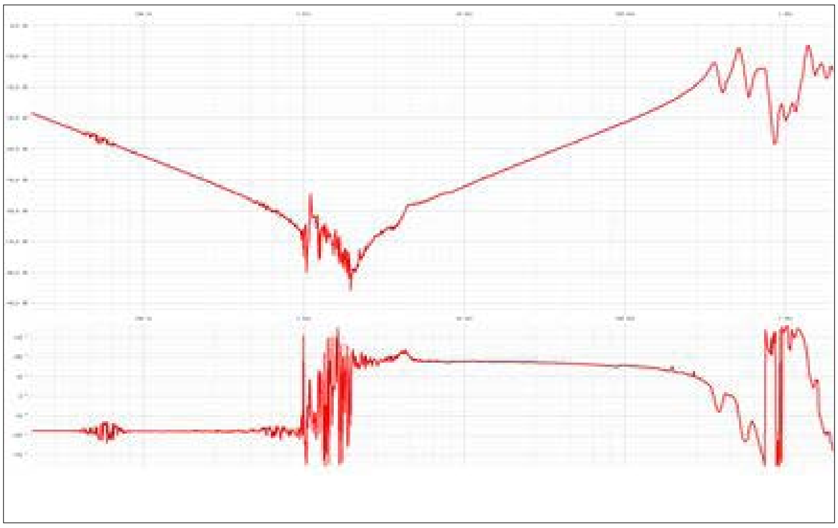

Figure 11. Effect of a bad dynamic range

Table 1. The effect of residual magnetism

After DC test	After demagnetization test
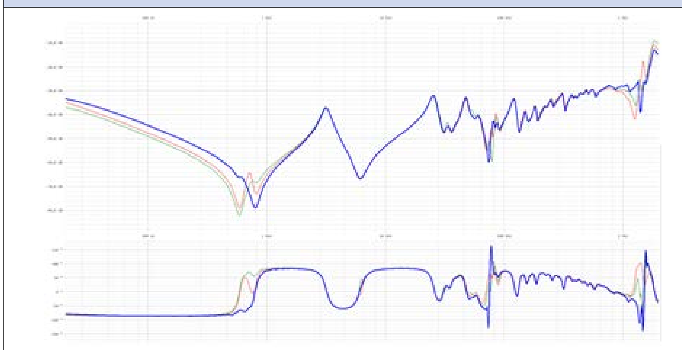	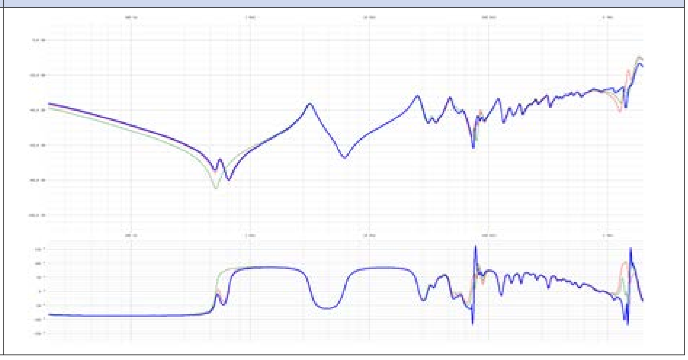

The prediction of the transformer state, more precisely the remanence level, is limited to three-phase transformers because the most significant deviation of all three phases has been used as a feature

The supervised machine learning multi-class classification approach was used for the predictions. Machine learning can be categorized in the artificial intelligence category as seen in Fig. 12. Furthermore, a grid search cross-validation for each model (k-nearest neighbours, decision tree, random forest, gradient boosting machine and support vector machine) was used to find the best parameter set for each machine learning model as well as the best model [9]. In the further course, the test and training data split for the investigations was set to 30 %. For the classification of influencing factors such as (Noise 50 Hz, Noise Floor, and Remanence) mentioned above, a scheme for each of them was developed, which has three categories:

- OK (good data quality)
- Investigate (data quality is good enough to do an assessment, but could be better)
- Error (data is not usable for further assessment)

For the performance determination of the individual algorithms, the F1 score was used, which is very meaningful for data sets that are not one hundred per cent balanced in their classes. It should be added that the true positives, as well as the true negatives, represent the count of correct predictions, whereas the false negatives indicate the number of wrong predictions. The definition of the F1 score can be found in the following:

$$Precision = \frac{\#of\ True\ Positives}{\#of\ True\ Positives + \#of\ False\ Positives}$$

$$Recall = \frac{\#of\ True\ Positives}{\#of\ True\ Positives + \#of\ False\ Negatives}$$

$$F1\ score = 2 \cdot \frac{Precision \cdot Recall}{Precision + Recall}$$

4.1. Noise prediction

On the one hand, there is noise occurring around the rated frequency / harmonic frequencies, and on the other hand, there is noise caused by the dynamic range of the measuring device. For noise detection, significant parameters are extracted from the SFRA curves to reduce the number of used features. In addition to the number of peaks, the height of the peaks is also extracted from the curve areas that are interesting about the respective category. This means that a total of two parameters per noise category, such as the average height and the number of peaks, are needed for the prediction task. Of the total 19,787 SFRA training curves, 1,872 were used for supervised learning / grid search validation of the power frequency noise detection so that the classes are better balanced between each other. Each trace has been assessed by an expert. The distribution of the classes was as follows:

- OK - 870
- Investigate - 870
- Error – 132

Of the total 19787 SFRA training curves, 447 were used for supervised learning / grid search validation of the noise floor detection so that the classes are better balanced between each other. The distribution of the classes was as follows:

- OK - 179
- Investigate - 179
- Error - 89

The gradient boosting algorithm [9] showed the best performance for both noise identification algorithms, with a mean F1 score for the power frequency noise validation of 98.932 % and the noise floor validation of 99.259 %. The following parameters were optimized during the grid search cross-validation: min_samples_split, max_depth min_samples_leaf, max_leaf_nodes, n_estimators, learning_rate. Furthermore, the cv value was set to five so that five folds for each combination of parameters were performed.

4.2. Remanence prediction

The prediction of the transformer state, more precisely the remanence level, is limited to three-phase transformers

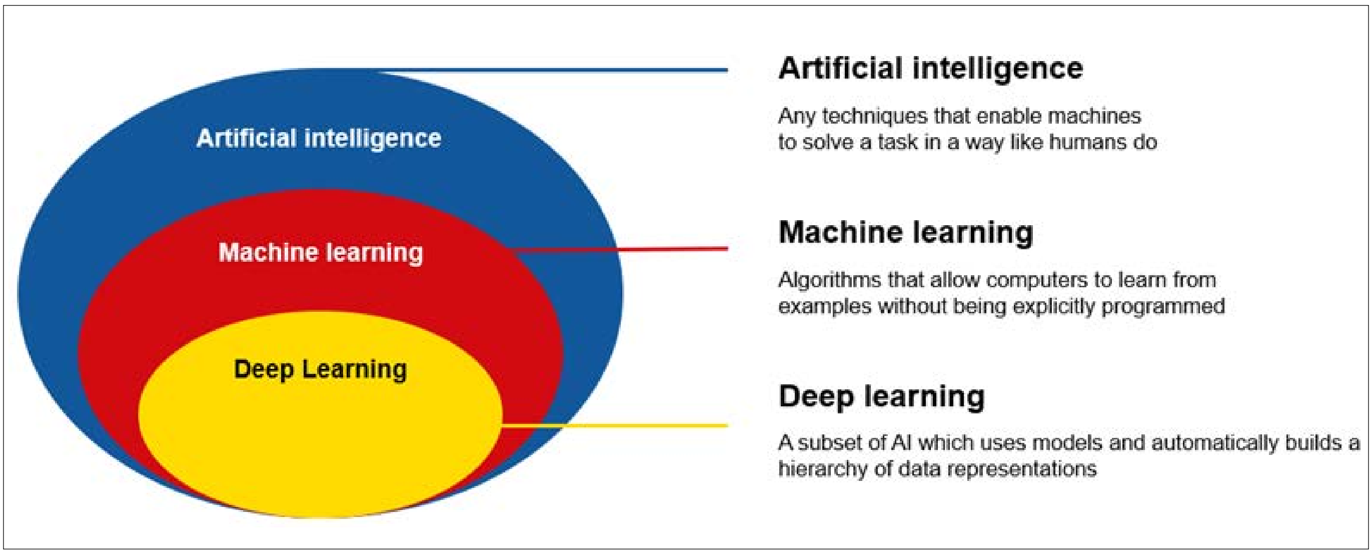

Figure 12. Artificial intelligence categories [9]

Table 2. Comparison of SFRA measurement types (20–30 kHz)

Measurement type	Nichols plot (scaled)	Nichols plot histogram (scaled)
End-to-End Open Circuit	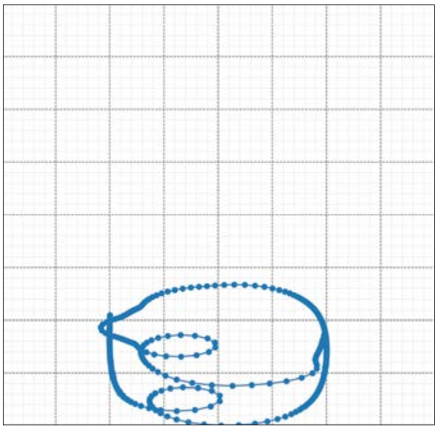 Figure 13. End-To-End Open Circuit	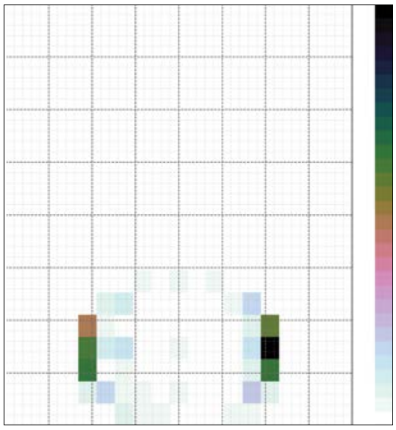 Figure 14. End-To-End Open Circuit
End-to-End Short Circuit	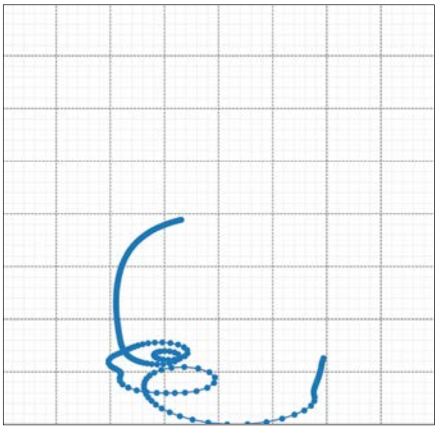 Figure 15. End-To-End Short Circuit	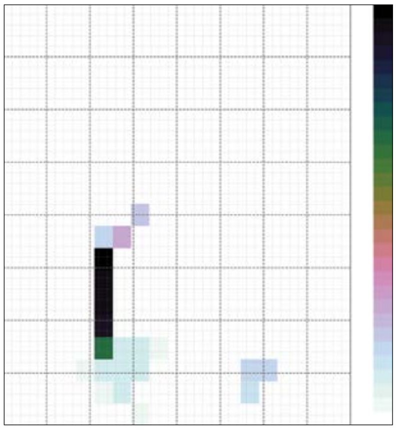 Figure 16. Nichols Histogram End-To-End Short Circuit
Capacitive Interwinding	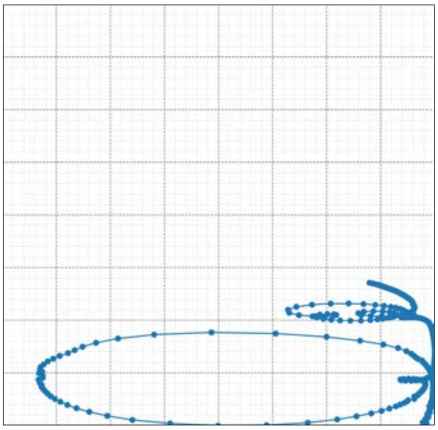 Figure 17. Capacitive Interwinding	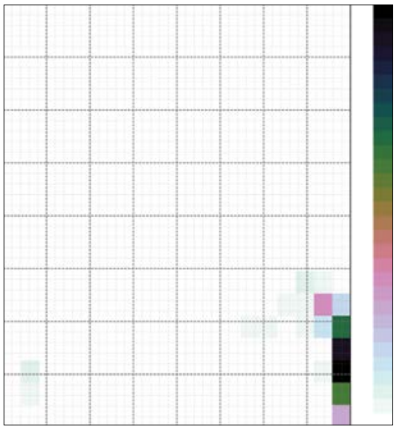 Figure 18. Capacitive Interwinding
Inductive Interwinding	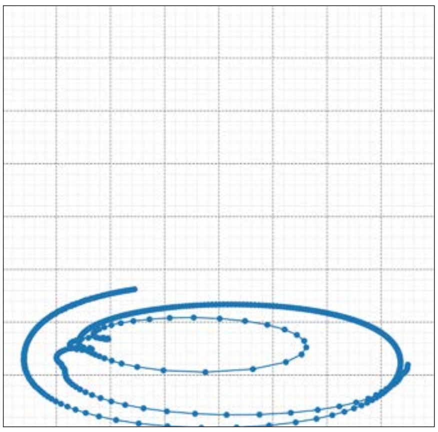 Figure 19. Inductive Interwinding	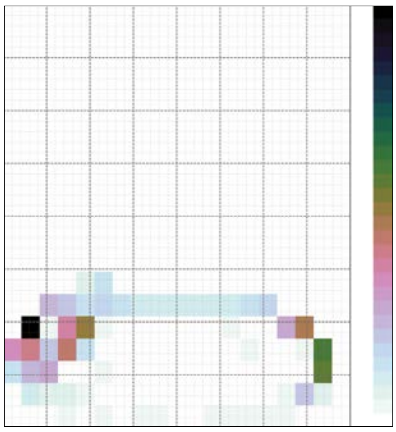 Figure 20. Inductive Interwinding

Cigre Working Group A2.26 introduced in 2008 ranges on the power transformers' MVA rating where the SFRA measurement should be evaluated

because the most significant deviation of all three phases has been used as a feature. Furthermore, all three phases of the HV End-To-End Open Circuit SFRA measurement are necessary. There is a clear difference visible in the lower frequency range up to about 10 kHz between the three curves if there is remanence in the power transformer, as in Table 1. For this prediction, several significant parameters were extracted, such as the area under the curves, the maximum deviation in percentage number at the beginning and the resonance point. The maximum cumulated area difference, the initial percentage deviation between the curves, and the maximum percentage deviation at the resonance between all curves are three examples. Of the total 2001 individual power transformers, SFRA measurements on 495 power transformers were used for supervised learning / grid search validation so that the classes are better balanced between each other. Each individual trace has been assessed by an expert. The distribution of the classes was as follows:

- OK - 203
- Investigate - 194
- Error - 98

The gradient boosting algorithm [9] for remanence prediction showed the best performance with an F1 score of 78.667 %. The procedure for this gradient boosting algorithm was the same as in section 4.1.

4.3. Pattern prediction of FRA measurement type

The individual SFRA measurement types are (see Fig. 13 [8] for connections schemes): Unknown, Calibration, End-To-End Open Circuit, End-To-End Short Circuit, Capacitive Interwinding and Inductive Interwinding. The curves are very much differentiating in both magnitude and phase, especially in the lower frequency band (below 30 kHz). The goal here is to try to assess this measurement type automatically by analyzing various parameters such as the coefficients of linear regression, a polynomial function, and histograms of a certain frequency and magnitude ranges, as well as the 3D SFRA [10] extracted. The 3D SFRA is an interplay between magnitude, phase and frequency where in this extraction, the frequency is neglected. A binning is performed based on the resulting nichols plot, from which a histogram is derived [10]. Each individual trace has been assessed by an expert.

The 3D SFRA method has been developed in this course to predict the pattern of SFRA traces. Table 2 shows the different standardized nichols plots per measurement type (min/max scaled) in the frequency range of 20 Hz to approx. 30 kHz due to an empirical analysis of more than 20.000 traces, which are distinguished by their measurement method as well as their pattern. Fig. 13 and Fig. 14 show examples of 2D histograms with binning, which are then processed by an algorithm (end-to-end open circuit measurements).

The gradient boosting [9] algorithm on nichols histograms included showed the best performance with an F1 score of 89.053 % to identify the type of FRA measurement.

5. Dynamic sub-band classification

Cigre Working Group A2.26 [8] introduced in 2008 ranges on the power transformers' MVA rating where the SFRA measurement should be evaluated. The Chinese standard NCEPRI [11] defines three frequency bands to evaluate according to the correlation coefficient. The lowest sub-band, where the core is dominating the characteristic of the curve is neglected by this evaluation algorithm. Juan Velasquez proposes in [12] to divide the SFRA trace into five parts (two lower frequency parts, one medium frequency and two higher frequency parts) as in the figure below. This proposed sub-band differentiation has the advantage that the magnetization inductance (Lm) and the parallel resonance with the parallel capacitance could be differentiated in the lower frequency range. Furthermore, the influence of the winding structure and the leads can be split.

Velasquez introduced an algorithm to find the different anchor points to differentiate the sub-bands [12]. The sub-bands of the lower frequency range could be split with a very good performance with the proposed algorithm. The differentiation between the MF and HF 1 sub-band still has a very high uncertainty with the proposed method, as the border was found by an empirical study.

The automatic sub-band identification of the MF as well as the HF1 sub-band, is very much dependent on the shape of the curve. It follows that the vector group, along with the MVA rating and the winding type, significantly impact the

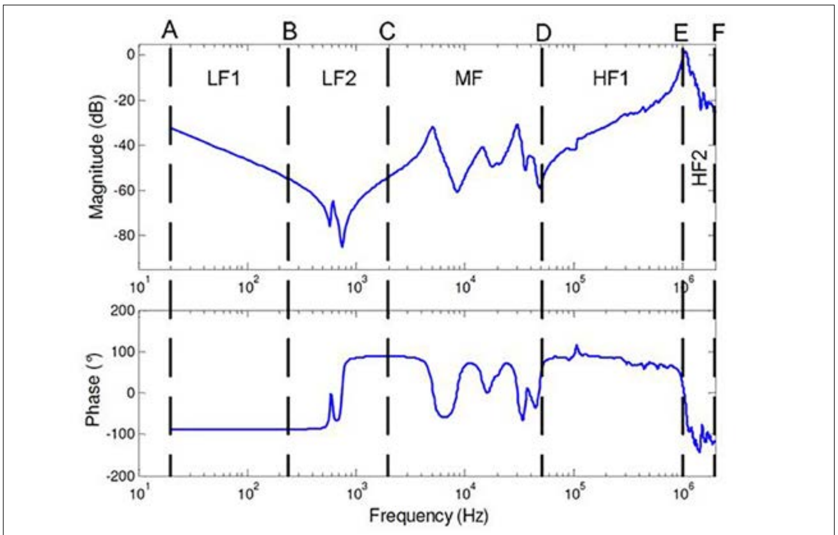

Figure 21. Proposed sub-bands [12]

The automatic sub-band identification of the MF as well as the HF1 sub-band, is very much dependent on the shape of the curve

Table 3 Comparison of high and low voltage winding types (30–600 kHz)

Winding type	Nichols plot (scaled)	Nichols plot histogram (scaled)
Continuous (HV)	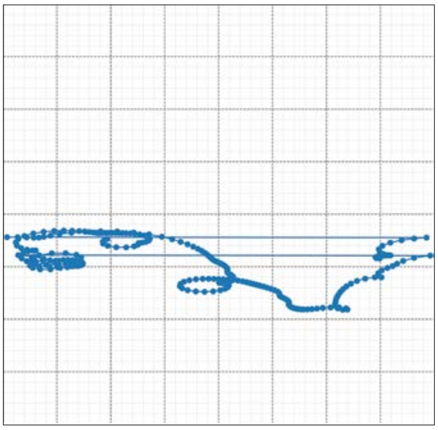 Figure 22. Continuous Disk Winding (HV)	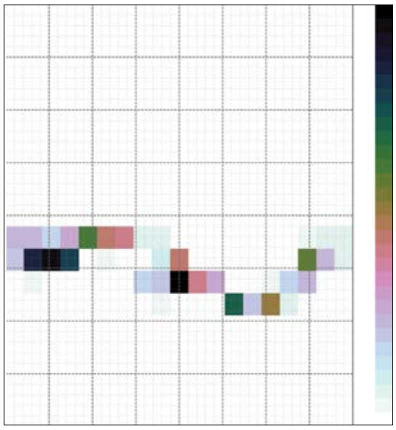 Figure 23. Continuous Disk Winding (HV)
CTC (HV)	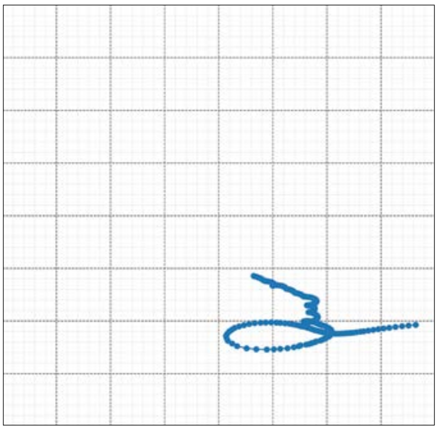 Figure 24. CTC Winding (HV)	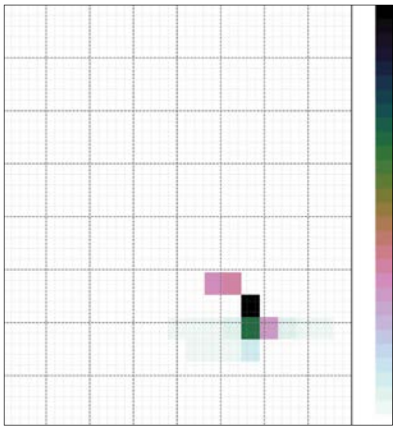 Figure 25. CTC Winding (HV)
Shielded (HV)	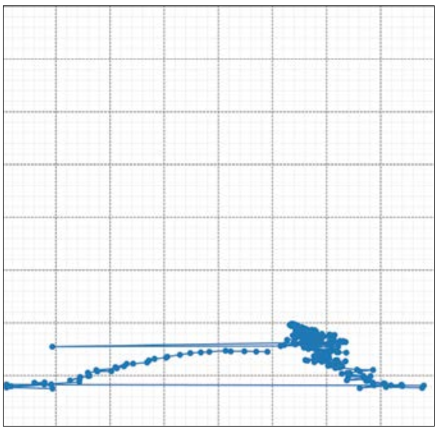 Figure 26. Shielded Continuous Disk Winding (HV)	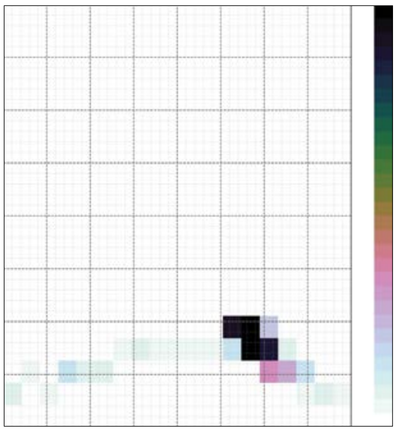 Figure 27. Shielded Continuous Disk Winding (HV)

More field cases are needed to understand better the possible correlations between transformer design, winding designs and SFRA patterns

boundaries of those bands. The vector group, including the MVA rating, is a kind of metadata which is provided by the respective SFRA software. The winding type is usually missing as this data is treated as important and confidential by the respective power transformer manufacturer. The first study on 17 different power transformers with different winding types showed that the winding type could be predicted with the use of the scaled nichols histograms (Table 3) and the gradient boosting algorithm.

The gradient boosting [9] algorithm with the nichols histograms showed the best performance with an F1 score of 85.137 % to identify the winding type. The procedure for this gradient boosting algorithm was the same as in section 4.1.

6. Conclusion

FRA assessments on transformers still require expert work most of the time. More field cases are needed to understand better the possible correlations between transformer design, winding designs and SFRA patterns, as demonstrated here, and it is always interesting to deepen those analyses.

On the other hand, machine learning algorithms, especially the gradient boosting algorithm, are more and more efficient and widely used to automatically assess significant parameters. Even if some expert work is needed to classify the validated FRAs on which those tools shall learn first, then the good results provided by those algorithms shall drive the development of even more FRA automatic assessments and improve their reliability.

Bibliography

[1] CIGRE Technical Brochure #642 WG A2.49, *Transformer reliability survey*, 2015

[2] CIGRE Technical Brochure #761 WG A2.49, *Condition assessment of power transformers*, March 2019

[3] A. Kraetge et al., *Aspects of the practical application of sweep frequency response analysis (SFRA) on power transformers*, 6th CIGRE South Africa Regional Conference, Paper P504, 2009

[4] CIGRE Technical Brochure #812 WG A2.53, *Advances in the interpretation of transformer Frequency Response Analysis (FRA)*, 2020

[5] J. Sanchez, *Classic power transformer windings*, Transformers Magazine, vol. 1, issue 2, 2014

[6] S. V. Kulkarni, S. A. Khaparde, *Transformer engineering design, technology and diagnostics*, 2nd edition, by CRC Press, 2013

[7] G. F. Stern, *Improvements in inductive windings*, Patent Specification 587,997; N°384/45, 1945

[8] CIGRE Technical Brochure #342 WG A2.26, *Mechanical condition assessment of transformer windings using Frequency Response Analysis (FRA)*, 2008

[9] A. C. Müller, S. Guido, *Introduction to machine learning with Python: A guide for data scientists*, translated from German by Kristian Rother, 1st edition, Heidelberg: O'Reilly, 2017

[10] A. Abu-Siada, R. Ibrahim, A. F. Abdou, *3D approach for fault identification within power transformers using frequency response analysis*, IET Science, Measurement & Technology 13, No. 6 (August 2019): 903–11, https://doi.org/10.1049/iet-smt.2018.5573

[11] NCEPRI, *Application guideline for transformer winding distortion test technology*, China 1999

[12] J. L. Velásquez Contreras et al., *Identification of transformer-specific frequency sub-bands as the basis for a reliable and automatic assessment of FRA results*, Conference on Condition Monitoring and Diagnosis 2010 (CMD2010), Tokyo (Japan), 6–11 September 2010

PEER REVIEWED

Authors

Jean Sanchez is a senior transformer engineer at EDF, a French main generation utility, mostly on investigations, tests and their associated diagnosis, FAT, HV bushings, and fleet assessments. He acquired PhD in power transformer fault diagnosis in 2011, with a French power transformer reparation factory.

David Gopp graduated with a master's degree in power engineering and energy management from the University of Applied Sciences in Dornbirn in 2019. He started his professional career as a working student at OMICRON electronics in software as well as hardware development. He then worked for two years as a technical support and applications engineer at OMICRON electronics, where he specialized in the evaluation and diagnosis of power transformers and instrument transformers. Since January 2020, he has been responsible for sweep frequency response analysis in product management. He is currently researching the implementation of algorithms to improve/automate the evaluation of SFRA measurements based on artificial intelligence.